

Molecular Identification of SqKv1A

A Candidate for the Delayed Rectifier K Channel in Squid Giant Axon

JOSHUA J. C. ROSENTHAL,* ROSS G. VICKERY,[†] and WILLIAM F. GILLY*

From the *Hopkins Marine Station, Department of Biological Sciences, Stanford University, Pacific Grove, California 93950; and [†]Department of Molecular and Cellular Physiology, Stanford University School of Medicine, Stanford, California 94305

ABSTRACT We have cloned the cDNA for a squid Kv1 potassium channel (*SqKv1A*). *SqKv1A* mRNA is selectively expressed in giant fiber lobe (GFL) neurons, the somata of the giant axons. Western blots detect two forms of SqKv1A in both GFL neuron and giant axon samples. Functional properties of SqKv1A currents expressed in *Xenopus* oocytes are very similar to macroscopic currents in GFL neurons and giant axons. Macroscopic K currents in GFL neuron cell bodies, giant axons, and in *Xenopus* oocytes expressing SqKv1A, activate rapidly and inactivate incompletely over a time course of several hundred ms. Oocytes injected with *SqKv1A* cRNA express channels of two conductance classes, estimated to be 13 and 20 pS in an internal solution containing 470 mM K. SqKv1A is thus a good candidate for the “20 pS” K channel that accounts for the majority of rapidly activating K conductance in both GFL neuron cell bodies and the giant axon. **Key words:** potassium channel • Kv1 • squid giant axon • inactivation

INTRODUCTION

Voltage-dependent potassium channels have been studied more extensively in the squid giant axon than in any other preparation. Mechanistic theories accounting for fundamental properties such as the ionic basis for action potential generation, voltage-dependent activation gating, (Hodgkin and Huxley, 1952) and open-channel block (Armstrong, 1969) were first developed in this preparation (Baker, 1984). Molecular analysis of K channels, however, has by-passed the squid.

The most intensively studied group of K channels on the molecular level are α -subunits of the Kv1 subfamily, whose representatives include splice variants of the *Drosophila Shaker* gene (Kamb et al., 1987; Schwarz et al., 1988; Pongs, 1992) and the closely related rat genes encoding RCK1-5 (Stühmer et al., 1989). Studies of mutated versions of these channels in heterologous expression systems have identified many specific amino acids and polypeptide domains that influence biophysical properties (Jan and Jan, 1992; Pongs, 1992). Other studies have revealed that the expression patterns of several Kv1 channels differ in regard to both cell type (Schwarz et al., 1990; Tsauro et al., 1992; Ribera and Nguyen, 1993; Mottes and Iverson, 1995) and subcellular distribution (Sheng et al., 1992; Wang et al., 1993;

Sheng et al., 1994; Wang et al., 1994; Klumpp et al., 1995; Mi et al., 1995).

Despite much progress, the functional properties of molecularly-identified K channels remain difficult to study in the specific neurons and subcellular domains in which they are expressed in vivo. Generally, this is due to the difficulties associated with complex populations composed of different types of neurons, any one of which may express a number of K channel subtypes. These problems can be reduced by turning to preparations that contain neurons identifiable as either an approximate monotype (e.g., Rohon-Beard cells in *Xenopus* embryos [Ribera and Nguyen, 1993] or bag cells in *Aplysia* [Quattrocci et al., 1994]) or on an individual basis (e.g., giant neurons in *Aplysia* [Pfaffinger et al., 1991]). Following this approach, we have reexamined the classical “delayed rectifier” potassium conductance (g_K)¹ in the squid giant axon and its monotypic cell bodies in the giant fiber lobe of the stellate ganglion (SG) to establish the molecular identity of the relevant K channels.

In this paper we describe a squid cDNA (SqKv1A) cloned from the stellate ganglion (SG)–giant fiber lobe (GFL) complex that encodes the α -subunit of a Kv1-type channel. To support the hypothesis that channels encoded by SqKv1A underlie macroscopic g_K in the gi-

Address correspondence to William F. Gilly, Hopkins Marine Station, Department of Biological Sciences, Stanford University, Pacific Grove, California 93950. Fax: 408-375-0793; E-mail: chipotle@leland.stanford.edu

¹Abbreviations used in this paper: GFL, giant fiber lobe; g_K , potassium conductance; I_K , potassium current; $[K_i]$, intracellular K concentration; $[K_o]$, extracellular K concentration; SG, stellate ganglion; utr, untranslated region.

ant axon system, we present results based on molecular, cell biological, and biophysical approaches. mRNA corresponding to the entire coding region of SqKv1A is expressed in GFL neuronal somata. SqKv1A channels are expressed in both the giant axon and GFL cell bodies. Functional properties of g_K from both cellular domains are consistent with one predominant channel type, and macroscopic and single SqKv1A channel currents recorded from *Xenopus* oocytes injected with SqKv1A cRNA are similar to those from giant axons and GFL neurons. Some of these results have been reported in preliminary form (Perri et al., 1994; Rosenthal et al., 1995; Mathes et al., 1996).

MATERIALS AND METHODS

Tissue Preparation

GFLs, SGs, and cleaned giant axons were dissected from adult *Loligo opalescens*. GFLs were separated from SGs at a point distal to their visually determined boundary for Northern blots, RNase protection assays, reverse transcriptase (RT)-PCR and Western blots. Giant axons for Western blots were manually cleaned in cold Ca-free artificial sea water (in mM: 480 NaCl, 50 MgCl₂, 5 KCl, 10 HEPES, pH 7.6) by separating away the small nerve fibers.

RNA Isolation

Total RNA (Chomczynski and Sacchi, 1987) was used to synthesize cDNA for RT-PCR. RNA for Northern blots was prepared by guanidinium thiocyanate lysis followed by LiCl precipitation (Rosenthal and Gilly, 1993). Guanidinium thiocyanate lysis followed by ultracentrifugation through CsCl (Sambrook, et al. 1989) was used to prepare RNA for RNase protection assays.

cDNA Library Screening

Approximately 10⁶ plaques from a lambda Uni-ZAP XR SG/GFL cDNA library (Rosenthal and Gilly, 1993) were lifted onto nylon filters (Hybond-N, Amersham Corp., Arlington Heights, IL) and hybridized with a ³²P-labeled probe made from pSKC-1 (see RESULTS) by random primer extension (Sambrook et al., 1989). Final washes were performed at high stringency (0.2× SSC [30 mM NaCl, 3 mM Na-citrate, pH 7] 65°C). One clone which contained the entire SqKv1A cDNA was plaque purified and excised in vivo into the bluescript II SK- phagemid (Stratagene Inc., La Jolla, CA). Nested deletions generated from both strands of SqKv1A with exonuclease III (Sambrook et al., 1989) were sequenced by

dideoxy chain termination (sequenase 2.0 kit; U.S. Biochemical Corp., Cleveland, OH).

PCR

Template DNA came from several sources, depending on the experiment. First-strand cDNA was synthesized from 1 μg total RNA with a cDNA cycle kit (Invitrogen Corp., San Diego, CA) using random hexamer primers. Lambda phage plaques in suspension medium (Sambrook et al., 1989) were incubated for 15' at 100°C. Miniprep plasmid DNA (~1 ng) was added directly to reactions.

Amplification conditions have been previously described (Rosenthal and Gilly, 1993), but in the present study the initial annealing temperature for reactions which used degenerate primers was 45°C instead of 37°C. Reactions were performed in a model 480 thermocycler (Perkin-Elmer Corp., Norwalk, CT) with the primers indicated in Table I (see also Fig. 1).

RNA Hybridizations

Northern blots and RNase protection assays using total RNA were performed as described previously (Rosenthal and Gilly, 1993). Probe sequences are given in the legend to Fig. 3. Undigested probe samples for RNase protection assays contained 1,000 cpm/lane. In situ hybridizations with frozen sections of fixed SG were carried out using a modified version (Liu and Gilly, 1995) of a standard protocol (Simmons et al., 1989).

Production of Polyclonal Antisera

Generation of polyclonal antisera was conducted in collaboration with Dr. S.R. Levinson, University of Colorado. A fusion-protein antigen containing NH₂-terminal SqKv1A sequence was constructed by PCR amplification of a cDNA fragment from SqKv1A plasmid DNA using primers SKC1 and SKC4 (Table I) that contained nucleotides 259 through 648 (aa 87-215) of the coding region. This product was cloned into the BamHI site of the prokaryotic expression vectors pRSET-B (Invitrogen Corp.) and pET-3B (Rosenberg et al., 1987) to yield pKC-SET and pKC-PET, respectively, and then transformed into *Escherichia coli* strain BL21 De3 pLys S. Fusion protein was induced in mid-log phase cultures by the addition of 0.5 mM IPTG. pKC-SET fusion protein was purified by nickel-affinity chromatography using Probond Resin (Invitrogen Corp.) according to manufacturer's specifications for denaturing conditions. pKC-PET fusion protein was purified by centrifugation of guanidinium thiocyanate cell lysates through 30% sucrose cushions (Rosenberg et al., 1987). Both pKC-SET and pKC-PET fusion proteins, which contain identical SqKv1A amino acid sequence, were used to inject New Zealand White rabbits. Antisera were purified over an affinity col-

TABLE I
List of Oligonucleotides

Oligo Name	Nucleotide Sequence	SqKv1A AA's	S/AS	SqKv1A Nucleotides
NEYFFD	AGTGAATTC AAYGARTAYTYTYYTGA	81-86	S	241-257
FWWAVV	GTCAAGCTTACNACNGCCACCARAA	359-364	AS	1075-1093
Skc-1	CACAGGATCCAGGGAATCGTCTAGTTTTGATGC	87-94	S	259-281
Skc-4	CAGGATCCTCATGTGCCAAATTTGGCATGG	210-215	AS	629-648
Skc-15	GCTGAGATCTGCCACCATGWTTAGAAAAGTTTCA	1-7	S	1-21
Skc-16	CATAAGATCTCAGACATCGGTTTGC	485-488	AS	1452-1469

Sequence nomenclature conforms to IUPAC conventions. Position of homologous SqKv1A amino acid (AA) or nucleotide sequence is indicated where relevant. S, sense; AS, antisense.

umn (Amino Link; Pierce Scientific, Rockford, IL) coupled to pKC-PET-generated fusion protein.

Western Blot Analysis

Western Blots were performed using standard protocols (Sambrook et al., 1989). GFLs and giant axons were homogenized in SDS-sample buffer (Sambrook et al., 1989). Approximately 10 μ g of protein was loaded on each lane of the gel. Affinity purified primary antibody was used at a dilution of 1:500. 125 I-conjugated goat anti-rabbit IgG (Amersham Corp.), at a dilution of 1:5,000, was used as secondary antibody. X-ray film (Kodak XAR-5) was exposed for 72 h at -70°C with one intensifying screen.

Construction of a *SqKv1A* Expression Plasmid

The entire coding region of *SqKv1A* was ligated to the 5' and 3' untranslated regions (utr) of the *Xenopus* β -globin gene by PCR with primers SKC-15 and SKC-16 (see Table I), which span the start and stop codons of *SqKv1A*. Primer SKC-15 changes the -3 nucleotide of *SqKv1A* from C to A to increase translational efficiency (Kozak, 1989). This product was cloned into the *Bgl*III site of plasmid pXOV (Wei et al., 1990) to create Chi-7. Regions synthesized by PCR were sequenced again.

Functional Expression of *SqKv1A* in *Xenopus* Oocytes

Plasmid Chi-7 was linearized with Not I, and capped cRNA was made with T7 RNA polymerase and the Message Machine Kit (Ambion Inc., Austin, TX). Approximately 25 ng of cRNA was injected per oocyte. Patch clamp recordings, conducted 2–4 d post injection, were performed in the cell-attached or inside-out configuration using a List LM-EPC7 patch clamp (Medical Systems, Greenvale, NY). Oocytes were bathed in a solution which contained (in mM): 140 KCl, 4.5 MgCl_2 , 10 EGTA, 10 HEPES, pH 7.3. Resting potentials of ~ 0 mV were confirmed on a subset of oocytes with intracellular recordings using micropipettes filled with 3 M KCl. Patch pipettes were from 1.5 to 4 M Ω . Solution compositions are given in the figure legends. Holding potential for all experiments, except where otherwise noted (see Fig. 7 D), was -80 mV. Temperature was 17 – 18°C . Data signals were filtered at 5 kHz (macroscopic experiments) or 0.5 kHz (single channel experiments) with an 8-pole Bessel filter before sampling with a 16 bit A-D converter at a rate of either 20 kHz or 2 kHz. Linear ionic and capacity currents for all macroscopic potassium current (I_K) records were removed on-line with a "P/-4" procedure.

Recordings from GFL Neurons

Whole-cell and outside-out patch recordings from isolated GFL neuron cell bodies of *Loligo opalescens* were carried out within 1 d of dissecting and plating in 35-mm culture dishes as previously described (Gilly et al., 1990). Holding potential was -80 mV and temperature was 18°C unless otherwise noted. Outside-out patch recordings used the same apparatus and procedures as those used in the oocyte experiments, and solutions are given in the figure legends. Procedures and the apparatus for whole-cell recordings were conventional (Gilly et al. 1990). The effective pipette resistance after conventional electronic compensation was <0.5 M Ω . Filtering was at 10 kHz, and sampling was carried out at either 20 kHz or 2 kHz. The external solution contained (in mM): 480 NaCl and 20 KCl (alternatively 430 NaCl and 70 KCl) plus 10 CaCl_2 , 10 MgCl_2 , 10 MgSO_4 , 10 HEPES (pH 7.6, 980 mosm). TTX was added from a frozen stock (10^{-4} M) to a final concentration of 200 nM. The internal solution contained (in mM): 20 KCl, 80 K-glutamate, 50 KF, 381 glycine, 291 sucrose, 3

lysine, 10 HEPES, 1 EGTA, 1 EDTA, 5 tetramethylammonium hydroxide (TMA-OH) (pH 7.0, 970 mosm).

Recordings from Perfused Giant Axons

Cleaned giant axons of *Loligo pealei* were internally perfused and voltage clamped using conventional axial-wire techniques (Gilly and Armstrong, 1982). Unfiltered data signals were sampled at 50 KHz. The external solution contained (in mM): 380 NaCl, 50 KCl, 38 CaCl_2 , 14 MgSO_4 , 10 HEPES (pH 7.2, 980 mosm). The internal solution contained (in mM): 50 KF, 3 lysine, 10 HEPES, 450 glycine, 450 sucrose, 1 EGTA, 1 EGTA and was titrated to pH 7.2 with TMA hydroxide. MgATP was added as described above before each experiment.

In all recordings described in this paper, small liquid-junction potentials exist to a varying degree between the different internal and external solutions and affect measurement of membrane voltage. These potentials were estimated to be <10 mV (inside with respect to outside) and have been ignored.

RESULTS

Delayed K Conductance in Giant Axons versus GFL Cell Bodies

At the outset of this study it was necessary to postulate the molecular identity of the delayed rectifier K channels in the giant axon and to question the relationship of these channels to those in the GFL somata, the presumptive site of channel synthesis in the system. A 20 pS channel underlies the bulk of g_K in GFL neuron somata and giant axons, and activation properties are very similar in both domains (Llano and Bookman, 1986; Perozo et al., 1991; Nealey et al., 1993). The rapid opening kinetics after a pronounced delay and very steep voltage dependence characteristic of squid g_K most closely resemble the functional properties of the *Kv1* subfamily of K channel α -subunits (Wei et al., 1990). Therefore we based our cloning strategies on this tentative identification.

Inactivation properties were not considered useful for the above comparison, because they are extremely variable, even among very closely related *Kv1* channels (Stühmer et al., 1989). Additionally, the relationship of the K channels in the giant axon to those in GFL neurons in regard to inactivation is unclear. Although the voltage-dependence of steady-state inactivation is very similar in both domains (Llano and Bookman, 1986; Clay, 1989; Perozo et al., 1989), kinetics of inactivation have been reported to differ significantly. Whereas even modest depolarizations lead to pronounced inactivation within several hundred ms in cell bodies (Llano and Bookman, 1986), no such "fast" inactivation has been detected in giant axons (Clay, 1989).

This discrepancy is clearly important to understanding the relationship between axonal and somatic 20 pS channels. We therefore reexamined inactivation kinetics in perfused giant axons, under experimental conditions that are conducive to robust inactivation in GFL

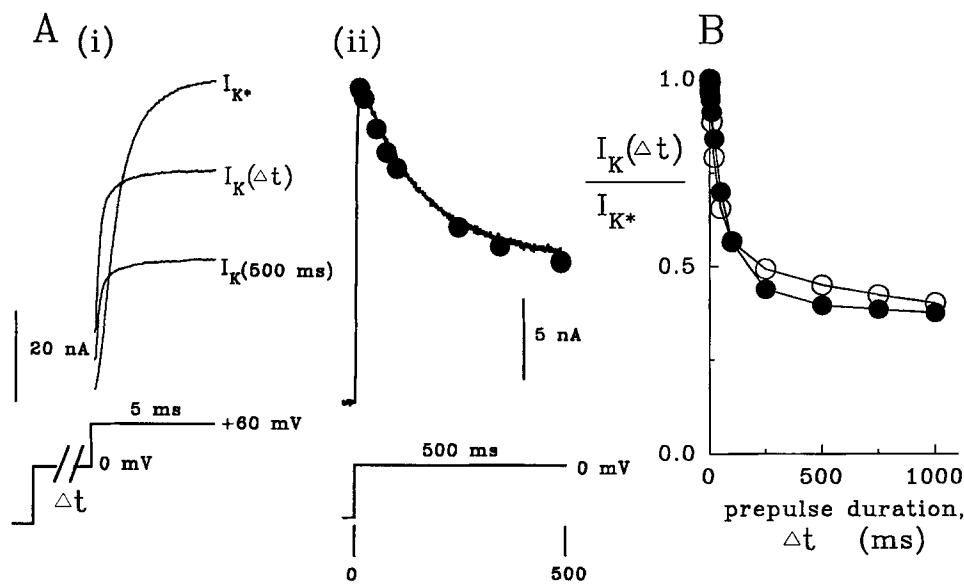


FIGURE 1. Comparison of inactivation kinetics of g_K in GFL neurons and giant axons. (A) (i) Examples of I_K in a GFL neuron at +60 mV are illustrated after prepulses to 0 mV for durations of 0.3 ms (I_{K^*}), 100 ms ($I_K[\Delta t]$), and 500 ms ($I_K[500 \text{ ms}]$). Whole-cell recording, (20 mM K_o , 12°C). (ii) Values of $I_K(\Delta t)$ (●) from the experiment in *i* are compared with the time course of I_K recorded directly during a long pulse to 0 mV in the same cell (12°C). $I_K(\Delta t)$ values have been scaled by the ratio of peak I_K at 0 mV to I_{K^*} . (B) Normalized $I_K(\Delta t)$ values, obtained at 18°C with prepulses as described in A, are illustrated for another GFL neuron (0 mV, 70 mM K_o) and for a perfused giant axon (axial wire clamp, -7 mV, 50 mM K_o).

neurons, by using a prepulse protocol (Fig. 1 A, inset) designed to avoid external K accumulation and polarization of the axial wire. Axons were stepped from -80 mV to a depolarized K reversal potential (V_K) level (set by adjusting extracellular K concentration ($[K_o]$) and intracellular K concentration ($[K_i]$) for varying durations in order to induce inactivation in the absence of I_K . Available I_K was assayed at the end of each prepulse ($I_K[\Delta t]$) with a brief test pulse to +60 mV and compared to maximum I_K after a very short prepulse (I_{K^*}). Because K accumulation is not a serious problem with whole cell recordings in GFL neurons, a similar two-pulse procedure could be used at voltages other than V_K .

Fig. 1 A*i* shows results on a GFL neuron cell body with prepulses to 0 mV for 0.3 ms (I_{K^*}), 100 ms ($I_K(\Delta t)$), and 500 ms. Inactivation kinetics thus determined with a series of prepulses (●) is compared in Fig. 1 A*ii* with the time course of inactivating I_K at 0 mV observed directly during a long pulse, and agreement between the two procedures is very good. Results of the two-pulse protocol from another GFL neuron (●) at 18°C are compared in Fig. 1 B with those obtained from a giant axon at (○) under similar conditions. In both, ~50% of the available g_K inactivates within 150 ms. Similar results were obtained on three other axons (12 and 18°C) and a large number of GFL neurons (3 at 18°C; 10 at 12°C). The absolute amount of inactivation in both axons and GFL cells is somewhat variable, and typically inactivation is more complete in GFL neurons. From these experiments we conclude that a significant fraction of g_K inactivates in both GFL neurons and giant axons at a similarly rapid rate, consistent with the idea of a single 20 pS channel type.

Cloning of a Squid K Channel cDNA

To clone the cDNA encoding the squid K channel discussed above, we focused on the GFL-portion of the SG, because only these neurons fuse to form the giant axons. RNA was selectively isolated from GFL neurons for use in RT-PCR using degenerate primers NEYFFD and FWWAVV (Table I), designed from amino acid sequence highly conserved among Kv1 channels. These primers span a region from the putative association domain (Li et al., 1992) to directly before S6 (aa 138-433, Fig. 2). A cDNA fragment of a size similar to that predicted (~850 bp) was amplified from GFL cDNA, cloned, and sequenced. The deduced amino acid sequence for this clone, pSKC-1, showed clear homology with Kv1 channels.

To isolate the full-length cDNA corresponding to pSKC-1, a SG/GFL cDNA library was screened under high stringency with probe synthesized from pSKC-1. 69 positives were isolated. Clones sufficiently large to contain the entire coding region expected for a typical Kv1 channel were identified by PCR from cored, positive plaques using primer SKC-4 (made from pSKC-1 sequence; Table I) and the T3 primer (from the vector). One of these clones, SqKv1A, which contains an insert of 2,067 nucleotides, was sequenced to completion.

SqKv1A mRNA consists of 503 bases of 5' untranslated sequence (utr), 121 bases of 3' utr and an open reading frame of 1,463 bases. The methionine codon at position 1 was designated as the start codon, because it produces the longest open reading frame. Nucleotides surrounding this codon (GTGATGT), in particular the pyrimidine at position -3 and the thymidine at posi-

SqKv1A	N-----F-----LKNPDE-----NNQLDAGSGSSHMCKR-----SDRVV	9
Shaker B	MAAVAGLQYLGEDRQHRKQKQQQQQHKRQLEQRKPEQKAIARKRLQLRQ	50
	-[P]R-[S]LQ-----LKNPDE-----NNQLDAGSGSGSSHMCKR-----SDRVV	43
	GLPRLSLLDGYGSLPKLSSQDEEGGAGHGFGGQPPQHPFPIP HDHDFCRVYI	100
	INVSGLRFPETQFRRLSQQFPD TLLQMPKRRNRYMDPVNNEYFFQGNRPSFD	93
	INVSGLRFPETQFRRLSQQFPD TLLQMPKRRNRYMDPVNNEYFFQGNRPSFD	150
	AILVYHSGGRLRRPQNVPLDIPLEETIRFRELQREVVTDKRYDAKSGPVMKEV	143
	AILVYVQSGGRLRRPQNVPLDIPLEETIRFRELQREVVTDKRYDAKSGPVMKEV	200
	EKPLPNDPQRLVWLLVHPKSSTPARVIAIVSVIVVIVISIVVFCLETLF	193
	EKPLPNDPQRLVWLLVHPKSSTPARVIAIVSVIVVIVISIVVFCLETLF	250
	EFKRVYELLNDTNGTKIIEEDAMFKPPTFFLIRTCGIIWFTMSEULIRFAS	239
	EFKRVYELLNDTNGTKIIEEDAMFKPPTFFLIRTCGIIWFTMSEULIRFAS	300
	CPKRLDFPKDQSHNAIDVVSITMPYFTTLQIVTQNDTNTQD-----	278
	CPKRLDFPKDQSHNAIDVVSITMPYFTTLQIVTQNDTNTQD-----	350
	SSNQMSLAIIRVIRLVRFVRFKLSRHSRGLQIQGLFKASRLRELGLLI	326
	SSNQMSLAIIRVIRLVRFVRFKLSRHSRGLQIQGLFKASRLRELGLLI	400
	FFLVIGVVLVSSAVYFARVDTQSHMFKSIFDFFWMAVVTMTTVGYGDMHIF	376
	FFLVIGVVLVSSAVYFARVDTQSHMFKSIFDFFWMAVVTMTTVGYGDMHIF	450
	VGVVGRLLVGS LCATAGVLTIALPVPVIVSNPNVYVYHRDABATGDRKRFQ	425
	VGVVGRLLVGS LCATAGVLTIALPVPVIVSNPNVYVYHRDABATGDRKRFQ	500
	NVLS-----ATNYVDEKISIVTSRVSISDIMEHDEG-----	455
	NVLS-----ATNYVDEKISIVTSRVSISDIMEHDEG-----	550
	VAPFLGAQQQQQQQPVASSLSMYSIKKKEGMLDNTNNI-----	473
	VAPFLGAQQQQQQQPVASSLSMYSIKKKEGMLDNTNNI-----	600
	QQNSFN-----QTQQQLQQQSHDINASAAAATGGSSGLTKRMHALLAV	482
	QQNSFN-----QTQQQLQQQSHDINASAAAATGGSSGLTKRMHALLAV	650
	SMQNDV 488	
	STRPDV 657	

FIGURE 2. Alignment of the predicted amino acid sequence for SqKv1A and Shaker B1. Boxed residues are identical. Solid lines are above putative membrane spans. Sites for protein kinase C-dependent phosphorylation and asparagine-linked glycosylation in SqKv1A are indicated by circled P's and G's, respectively. The alignment was made using the Geneworks software suite (Intelligenetics, Mountain View, CA). The Genbank accession number assigned to the SqKv1A nt sequence is U50543.

tion +4, do not constitute a favorable context for translational initiation (Kozak, 1989); however, no other potential translational start site contains a more favorable context. An in-frame stop codon occurs at position 1,967, directly following sequence encoding the highly conserved T(D/E)V amino acid motif at the COOH terminus of Kv1 channels. A polyadenylation signal (Proudfoot and Brownlee, 1976) at positions 1539–1544 terminates the short 3' utr.

Protein Structure

SqKv1A mRNA encodes a protein of 488 amino acids (55.7 kD). A Kyte-Doolittle (Kyte and Doolittle, 1982) hydropathy plot (not illustrated) is consistent with the generally accepted K channel structure. Based on amino acid sequence homology, SqKv1A is most closely related to Kv1 subfamily members and shows a lower degree of conservation with Kv2, Kv3, and Kv4 channels. Naming of SqKv1A is meant to indicate that it is the first squid Kv1 gene described. The predicted amino acid sequence of SqKv1A is compared with that of Shaker B in Fig. 2. Homology is strongest in the channel core region. Membrane spans S4–S6 and the pore, believed to regulate many properties of activation gating and permeation, are nearly identical. Amino acid similarity is greatly reduced at both the NH₂ and COOH terminals, and the squid sequence is significantly shorter in each of these domains.

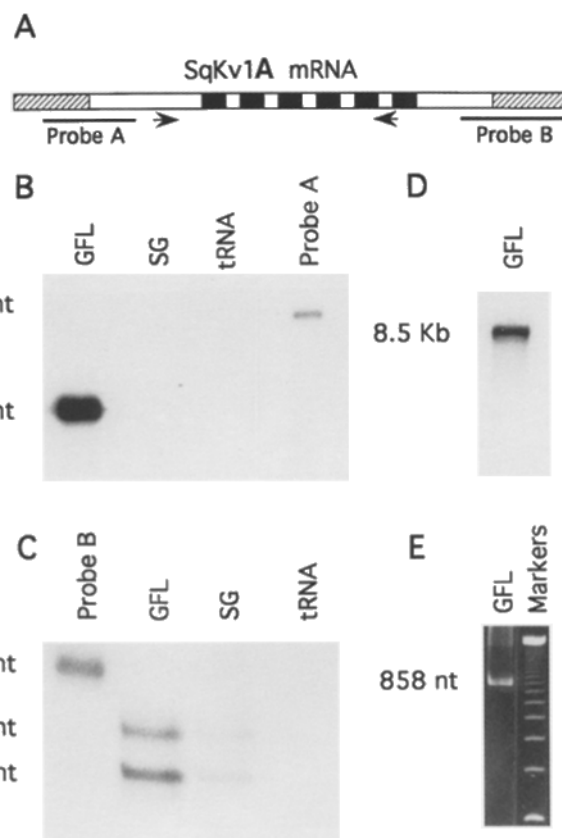
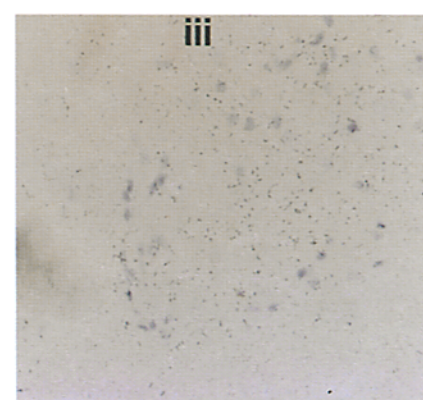
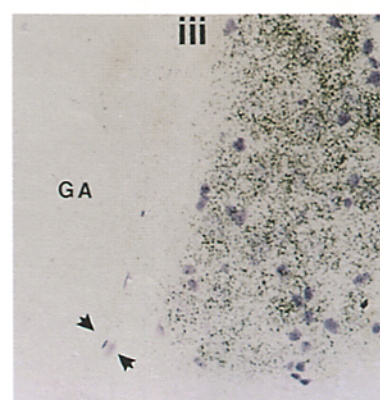
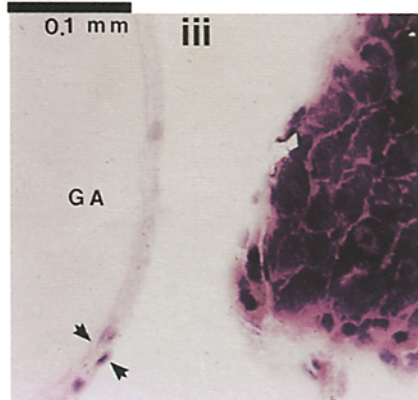
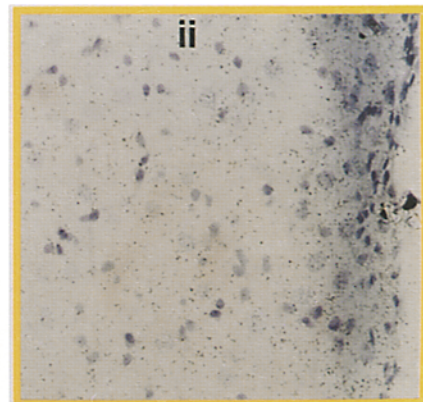
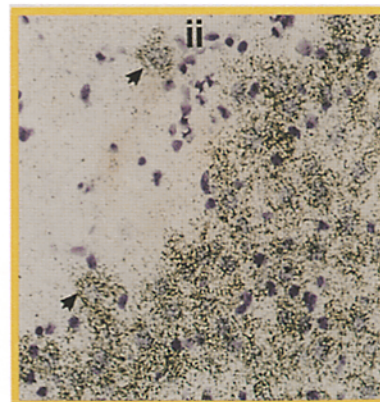
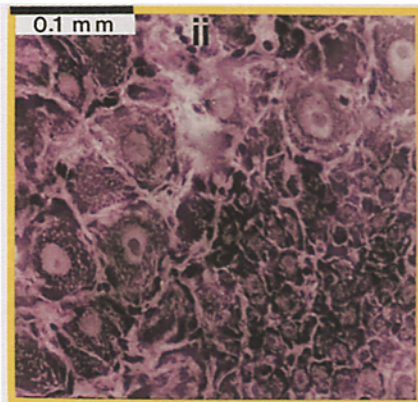
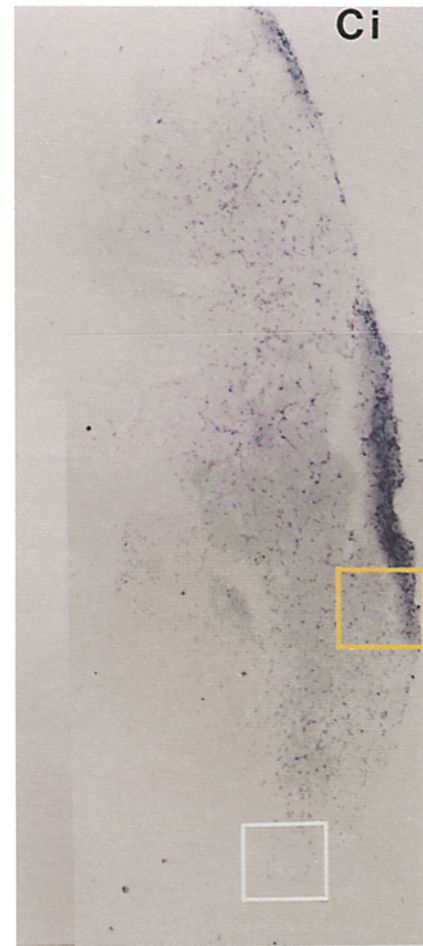
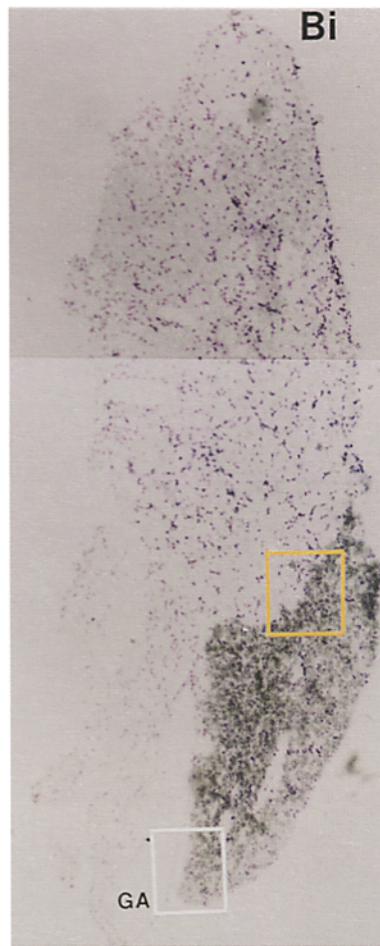
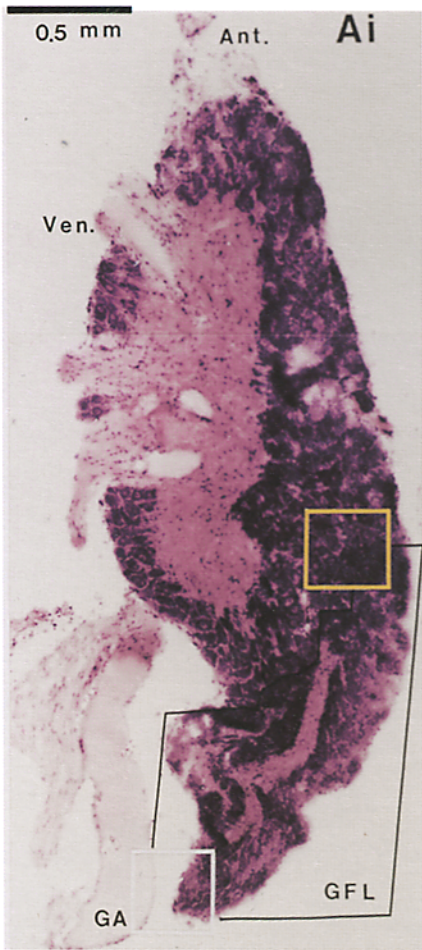


FIGURE 3. Expression of SqKv1A mRNA within the stellate ganglion. (A) Linear depiction of the SqKv1A mRNA. Solid regions indicate membrane spans, and cross-hatched regions indicate untranslated sequence. Approximate positions of probes and PCR primers (arrows) are given. (B) RNase protection assay using probe A (nucleotides -103 to +101 of SqKv1A). (C) RNase protection assay using probe B (nucleotides 1146–1586 of SqKv1A). (D) Northern blot using probe B. (E) PCR of cDNA made from GFL RNA using primers NEYFFD and FWWAVV (see Table I). Markers are 123 bp ladder (Gibco). tRNA samples (10 g) were included in RNase protection assays as controls for nonspecific binding. GFL, giant fiber lobe RNA sample. SG, stellate ganglion (without GFL) RNA sample.

The NH₂ terminus of SqKv1A (i.e., amino acids 1–15) is unusually hydrophobic for a Kv1 channel, but the functional significance of this feature is unknown. Although four scattered basic residues (aa 3,4,12,17) exist in this region, followed by four closely spaced acidic residues (aa 20–22,27), this arrangement bears only rough similarity to the well-defined inactivation “ball and chain” sequence of Shaker B (Hoshi et al., 1990) or even to the more general features found in RCK4 (Tseng-Crank et al., 1993). Other members of the RCK group which show little inactivation lack positively charged amino acids in this region entirely, however (Stühmer et al., 1989).

Consensus sites for N-linked glycosylation occur at N202 in the S1-S2 extracellular loop and at N272 and N281 in the S3-S4 loop. Typically Kv1 channels contain



only 1 or 2 glycosylation sites found exclusively in the first extracellular loop. Two highly conserved protein kinase C-dependent phosphorylation sites are present in SqKv1A at T314 and S318. Two nonconserved sites, S39 and T459, occur at the NH₂-terminal and COOH-terminal cytoplasmic domains, respectively. SqKv1A contains no consensus sites for cyclic adenosine monophosphate dependent phosphorylation.

Expression of SqKv1A in GFL Neurons

RNA isolated from the entire SG was used to construct our cDNA library (Rosenthal and Gilly, 1993). Although GFL neurons constitute a large proportion of the SG (see Fig. 4 *Ai*), many other types of neurons are present. To positively identify SqKv1A with the giant axon system, expression of SqKv1A mRNA in GFL neurons was confirmed with four separate techniques, three of which used RNA selectively isolated from GFL tissue (Fig. 3).

First, Northern blot hybridization using a probe that contained 3' coding and utr sequence (Fig. 3 *A*, *Probe B*) revealed a band of ~8.5 kb (Fig. 3 *D*). Similarly large messages exist for other Kv1 channels from invertebrates (Pfaffinger et al., 1991; Schwarz et al., 1988) and for a squid Na channel (Rosenthal and Gilly, 1993).

Second, to evaluate more critically the identification of SqKv1A mRNA in GFL neurons, RNase protection assays were used to test whether exact sequence corresponding to both ends of SqKv1A mRNA is expressed in GFL neurons. Separate probes, one containing 5' utr and NH₂-terminal coding sequence (Fig. 3 *A*, *Probe A*) and a second containing 3' utr and COOH-terminal coding sequence (Fig. 3 *A*, *Probe B*), were assayed with GFL RNA. Fully protected bands of 204 nt for probe A (Fig. 3 *B*) and 438 nt for probe B (Fig. 3 *C*, *upper band*) were detected, confirming the presence of both 5' and 3' coding regions for SqKv1A mRNA in this tissue. Probe A hybridizes only with GFL RNA, whereas probe B hybridizes with both GFL and SG RNA (See DISCUSSION). The doublet seen in Fig. 3 *C* is an artifact of the probe and does not reflect alternative forms of SqKv1A as evidenced by an RNase protection assay using in

vitro-transcribed SqKv1A cRNA in place of GFL RNA, which yielded the identical banding pattern (data not shown).

Third, presence of the SqKv1A core region in GFL mRNA was demonstrated by PCR amplification with degenerate primers NEYFFD and FWWAVV (Fig. 3 *E*). The sequence of the cloned amplification product from this reaction (pSKC-1) was identical to that of SqKv1A. Because utr regions are generally highly variable, and the entire SqKv1A cDNA was isolated from a single lambda phage clone, it is extremely likely that this entire mRNA is expressed in GFL neurons. Of course, the presence of alternatively spliced versions of SqKv1A mRNA in GFL neurons cannot be entirely ruled out.

Finally, in situ hybridization methods were used to localize SqKv1A mRNA expression within the SG. Fig. 4 *Ai* is a stained vertical section (i.e., lateral view) of a SG and attached GFL. A large mass of neuropil in center of ganglion (*pink*) is surrounded by cell bodies of neurons (*dark purple*). A black border indicates the GFL portion of the SG. Within this lobe tracts of merging axons of GFL neurons (which fuse to form the giant axons) are stained pink. The largest, most posterior giant axon is indicated (*GA*). A higher magnification of the boundary zone between GFL cell bodies and those of SG proper (Fig. 4 *Ai*, *yellow box*) is illustrated in Fig. 4 *Aii*. A sharp border exists between the smaller GFL cells (*lower right*) and the larger ones of the SG. Nuclei of neurons appear to be stained a pale purple in comparison to the more intense purple-blue staining shown by smaller cells, presumably glial and/or capillary-forming endothelial cells. A higher magnification view of the posterior tip of the GFL and the adjacent giant axon is pictured in Fig. 4 *Aiii*. A thin layer of Schwann cells surrounding the axon is visible (*arrows*), and nuclei are confined to this layer.

Results of in situ hybridization with antisense probe for SqKv1A are shown in Fig. 4 *Bi-iii*, and analogous controls are presented in Fig. 4 *Ci-iii*. A low-power view of the ganglion (Fig. 4 *Bi*) reveals labeling only over the GFL region. Higher magnification of the boundary between GFL and SG cell bodies (Fig. 4 *Bii*) confirms this

FIGURE 4. Selective detection of SqKv1A mRNA in GFL neurons by in situ hybridization. (*A*) (*i*) Vertical section of a stellate ganglion with attached GFL and hind-most stellar nerve containing a giant axon. Staining is with basic fuchsin. (*ii*) Higher magnification of the yellow-boxed region of *Ai* showing the distinct boundary between SG and GFL neurons. (*iii*) Higher magnification of the white-boxed region of *Ai* showing the tip of the GFL and a portion of the adjacent giant axon (*GA*). (*B*) (*i*) Section of the same ganglion as above after in situ hybridization with radiolabeled, antisense probe for SqKv1A (probe A of Fig. 3 *A*). Staining of nuclei is with cresyl violet. SqKv1A mRNA is detected only in the GFL. (*ii*) Higher magnification (same as *Aii*) of the yellow-boxed region of *Bi* showing the SG-GFL boundary. (*iii*) Higher magnification (same as *Aiii*) of the white-boxed region in *Bi*. SqKv1A mRNA is not detectable in the giant axon (*GA*) or surrounding Schwann cells (*arrows*). (*C*) Control experiment carried out on a section from the same ganglion as above using a radiolabeled sense probe (same as used by Liu and Gilly, 1995). (*i*) Low-power view corresponding to *Bi*. The dark blue region on the dorsal surface represents a thicker region of the section and does not contain silver grains above background level (see also *Cii*). (*ii-iii*) Yellow- and white-boxed regions, corresponding to the SG-GFL boundary and GFL tip, are shown at higher magnification (same as *Bii* and *Biii*) in *Cii* and *Ciii*, respectively.

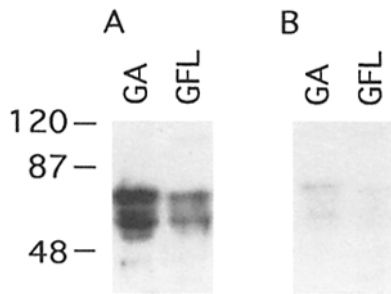


FIGURE 5. (A) Western blot of cleaned giant axon and giant fiber lobe tissue samples with anti-SqKv1A antibody. (B) A similar blot in which the primary antibody was blocked by preincubation with an equal volume of a solution of the fusion protein (1 mg/ml) against which the antibody was raised.

picture. Only occasional neurons separated from the mass of GFL cell bodies were labeled (*arrows*), and these were always close to the boundary. Labeling thus appears to be restricted to GFL neurons and is absent in the merging axon tracts within the GFL (Fig. 4 *Bi*), in the giant axon itself (Fig. 4 *Biii*, GA), or in the surrounding Schwann cell layer (Fig. 4 *Biii*, *arrows*). Thus within the SG, SqKv1A mRNA is expressed selectively, if not exclusively, in the subset of monotypic GFL neurons that form the giant axon.

SqKv1A Protein Is Expressed in the Giant Axon

Western blots were used to determine whether SqKv1A protein is expressed in the giant axon and therefore

could underlie axonal g_K . Polyclonal antisera were raised against, and affinity purified with, a bacterial fusion protein which contained NH₂-terminal SqKv1A amino acid sequence (amino acids 87–215; Fig. 2). Samples of giant axon, cleaned of the surrounding small nerve fibers, and of GFL tissue were processed for Western blot analysis. Bands of ~73 and 58 kD were evident in both the giant axon and the GFL samples (Fig. 5 *A*), and blocking controls confirm specificity of this result (Fig. 5 *B*). Although the smaller band is only slightly larger than the predicted core peptide, the 73-kD band is significantly larger. Any number of post-translational modifications such as glycosylation, phosphorylation, or fatty-acylation may account for this difference. Given the above results we conclude that SqKv1A protein is expressed in both GFL neuron somata and in the fused giant axons.

Functional Expression of SqKv1A

Injection of cRNA for SqKv1A into *Xenopus* oocytes results in the expression of rapidly activating, transient outward currents. These currents are identifiable as I_K by the appropriate dependence of reversal potential on $[K_o]$. They are relatively insensitive to extracellular tetraethylammonium, requiring >20 mM to achieve 50% block (data not shown).

Macroscopic I_K studied with cell-attached patch recordings on oocytes injected with SqKv1A cRNA were

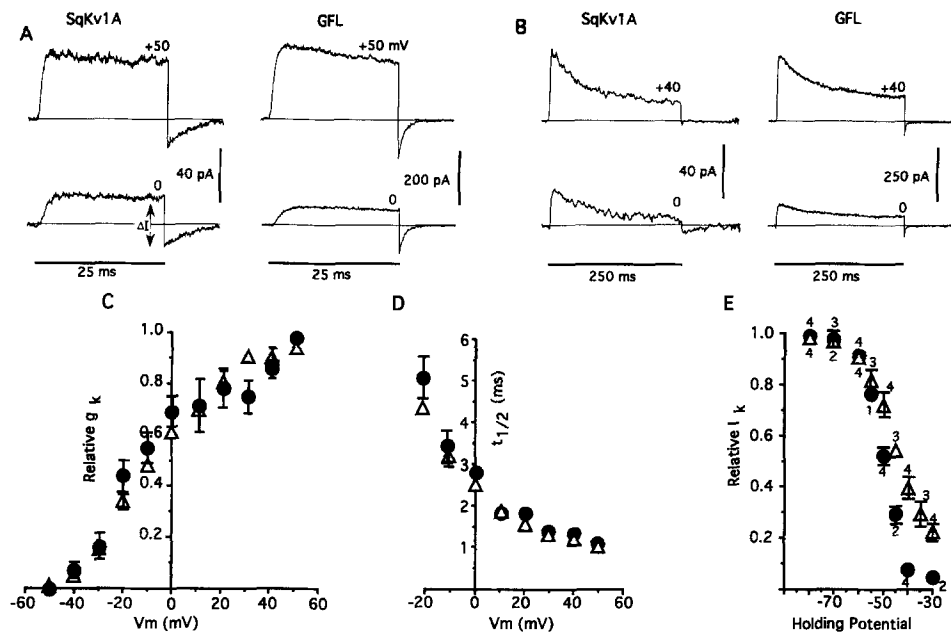


FIGURE 6. I_K in cell-attached patch recordings from *Xenopus* oocytes expressing SqKv1A and from GFL neurons. (A) I_K for 25-ms pulses to the indicated voltages. (B) I_K for 250-ms pulses to the indicated voltages. (C) Relative g_K vs. membrane voltage. g_K was measured as $(\Delta I/\Delta V_M)$ at the end of 25-ms pulses (see A), where ΔV_M is the amplitude of the activating pulse. Plotted g_K values were normalized to the maximum g_K value and represent means of three patches for both GFL neurons (Δ) and oocytes (\bullet). (D) Activation time to half-peak current ($t_{1/2}$) was measured for 25-ms pulses, and these values are plotted against V_M . Each point represents the mean of four patches. (E) Relative I_K vs. holding potential (HP). Patches were maintained at the indicated

HP for ≥ 1 min and then pulsed to +60 mV. Peak I_K at each HP was divided by the value of I_K at HP = -80 mV. Sample sizes (number of patches) are indicated next to each point. Only error bars (SEM) which are bigger than figure symbols are included. Oocytes were bathed in (in mM): 140 KCl, 4.5 MgCl₂, 5 EGTA, 5 EDTA, 10 HEPES, pH 7.2. Pipettes were filled with (in mM): 20 KCl, 120 NaCl, 4.5 MgCl₂, 5 EGTA, 5 EDTA, 10 HEPES, pH 7. GFL neurons were bathed in (in mM) 100 KCl, 400 NaCl, 10 MgCl₂, 10 MgSO₄, 10 CaCl₂, 10 HEPES, pH 7.4. Pipettes were filled with (in mM) 50 KF, 20 KCl, 310 K-Glutamate, 1 EGTA, 1 EDTA, 90 glycine, 90 sucrose, 5 Mg-ATP, 3 lysine, 10 HEPES, pH 7.4.

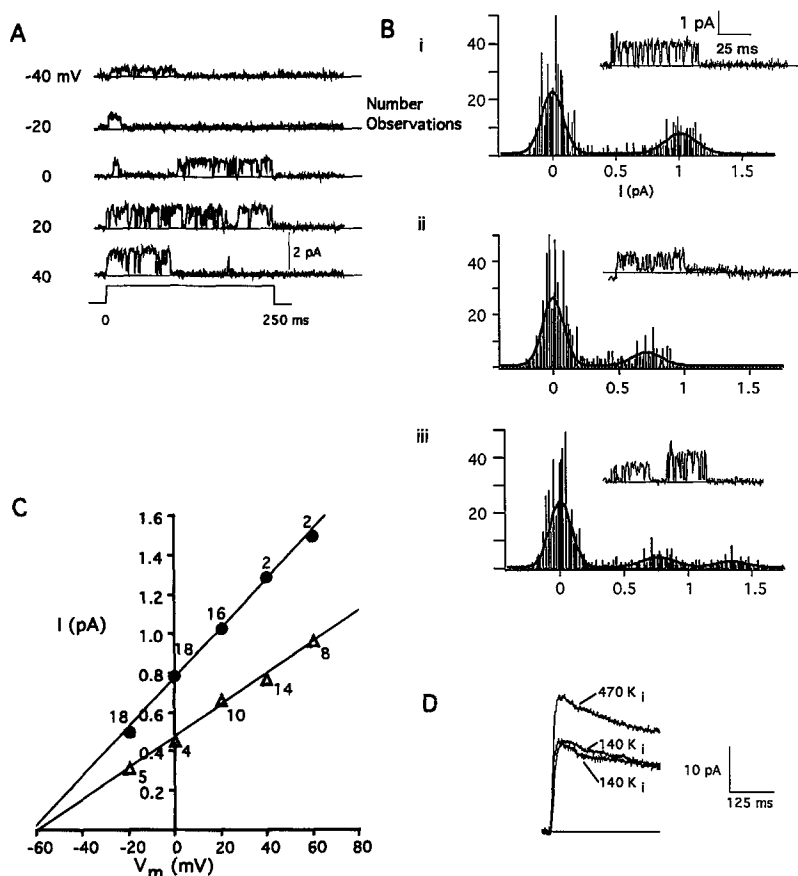


FIGURE 7. Single channel currents with two unitary conductance values recorded from excised inside-out patches from oocytes expressing *SqKv1A*. (A) Representative single channel records from a patch after 250-ms depolarizations to the indicated voltages. (B) Two unitary event amplitudes are evident within a single patch upon depolarization to +20 mV. Examples of large events (i), small events (ii), and mixed events (iii) are given. Accompanying each trace is an all-points histogram (bin width = 0.025 pA) with best fits to each peak as the sum of two or three Gaussian distributions (Igor Software; Wavemetrics Inc., Oswego, OR). (C) Determination of slope conductance for large events (●) and small events (△). Single sweep histograms (similar to those in B) were constructed from many sweeps to various voltages. Amplitudes of small events and large events at each voltage were estimated from Gaussian-fitted peaks, and mean amplitudes (n indicated next to each point) were plotted vs. V_M . Slope conductance was 12.5 pA for large events and 8.0 pA for small events (SEMs for each point were smaller than the symbols). (D) Derivation of a scaling factor to compare *SqKv1A* single-channel conductances recorded in oocytes with those reported from squid experiments. I_K at +40 mV was recorded from a GFL neuron (inside-out patch, 25-ms pulse from a holding potential of -80 mV) at 140 mM $[K_i]$ before and after changing the bath to 470 mM $[K_i]$. Similar experiments using pulses to +20, +40, and +60 mV were performed on three separate patches and slope conductance for each $[K_i]$ was calculated. A scaling factor of 1.6 ± 0.06 (mean \pm SEM) was thus determined for these values of $[K_i]$. Solutions and conditions for A–C were the same as those indicated for oocyte recordings in Fig. 6. The pipette solution for D was the same as the bath solution in Fig. 6 squid experiments, except it contained 10 KCl and 490 NaCl. 470 mM $[K_i]$ bath solution was (in mM) 50 KF, 20 KCl, 400 K-glutamate, 1 EGTA, 1 EDTA, 5 Mg-ATP, 3 lysine, 10 HEPES, pH 7.4. 140 mM $[K_i]$ was the same except for having 70 K-glutamate, 330 glycine, and 330 sucrose.

ductance for each $[K_i]$ was calculated. A scaling factor of 1.6 ± 0.06 (mean \pm SEM) was thus determined for these values of $[K_i]$. Solutions and conditions for A–C were the same as those indicated for oocyte recordings in Fig. 6. The pipette solution for D was the same as the bath solution in Fig. 6 squid experiments, except it contained 10 KCl and 490 NaCl. 470 mM $[K_i]$ bath solution was (in mM) 50 KF, 20 KCl, 400 K-glutamate, 1 EGTA, 1 EDTA, 5 Mg-ATP, 3 lysine, 10 HEPES, pH 7.4. 140 mM $[K_i]$ was the same except for having 70 K-glutamate, 330 glycine, and 330 sucrose.

compared to I_K measured in GFL neurons with excised, outside-out patches (Fig. 6 A). g_K from both preparations is extremely similar in regard to the voltage dependence of peak g_K (Fig. 6 C) and of activation kinetics (Fig. 6 D). Visual inspection of the records in Fig. 6 A reveals that deactivation kinetics are slower in *SqKv1A*-injected oocytes than in GFL neurons. Extensive tail data, however, are not yet available for *SqKv1A*-currents, and therefore this parameter was not examined in greater detail. Similarly slow tails at -80 mV have been observed in whole-cell recordings from GFL neurons maintained in culture for extended periods (e.g., 2 wk) as well as in excised patch recordings from cut-open giant axons, but the basis for this altered behavior is unknown (unpublished data).

Inactivation properties of K channels are also similar in GFL somata and *SqKv1A*-injected oocytes. Typically 40–80% of I_K in GFL neurons inactivates over 250 ms (Fig. 6 B; See also Llano and Bookman, 1986; Nealey et al., 1993), and cell-attached patch recordings from an oocyte expressing *SqKv1A* channels reveal a similar pattern (Fig. 6 B). The relationship between steady-state

inactivation and voltage, as determined by holding potential changes, is also comparable in *SqKv1A*-injected oocytes, GFL neurons (Fig. 6 E), and in giant axons (Clay, 1989; Perozo et al., 1989), but inactivation in the latter two preparations is always less complete.

Single-Channel Behavior of *SqKv1A* in Oocytes

Single channel recordings carried out from oocytes expressing *SqKv1A* channels lend further support to the idea that *SqKv1A* encodes the delayed rectifier K channel in the giant axon system. Fig. 7 A illustrates a family of records taken at different voltages. *SqKv1A* channels open rapidly in response to positive voltage steps, and display prominent bursting, a behavior characteristic of the native 20 pS channels in giant axons (Conti and Neher, 1980; Llano et al., 1988; Perozo et al., 1991) and GFL somata (Llano and Bookman, 1986; Nealey et al., 1993).

Surprisingly, our experiments also revealed that *SqKv1A* channel openings can show two distinct unitary amplitudes. Fig. 7 B shows three records from the same patch taken at +20 mV. Visual inspection indicates that trace

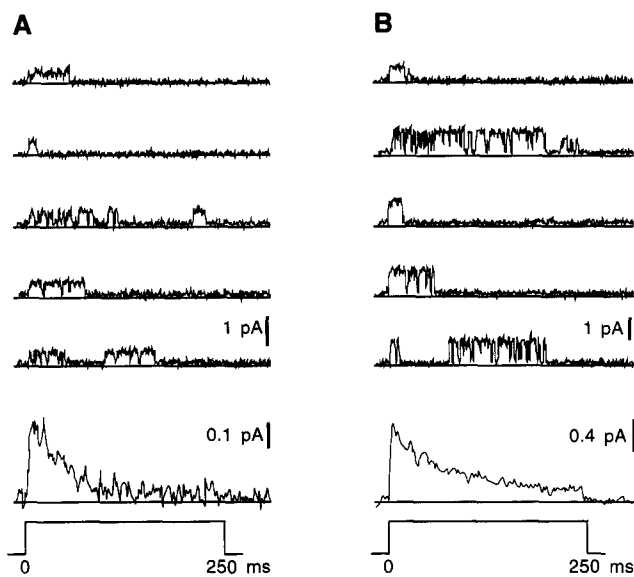


FIGURE 8. Ensemble averages from single channel events of SqKv1A channels recorded in cell-attached patches from oocytes. (A) Representative traces at +20 and the average of 30 such traces. This patch apparently contained a single active channel that exhibited only small conductance openings. (B) Representative traces at +20 mV from a patch containing two to three active channels and the average of 49 traces. Both large and small conductance events occurred in this patch but the majority of openings were large. Solutions are the same as those used for Figs. 6 and 7.

i contains a "large" conductance event, trace *ii* contains a "small" conductance event, and trace *iii* contains both. All-points histograms constructed from these traces support this conclusion. Histograms of this type were used to analyze sweeps at various voltages to determine the current-voltage relationships for large and small events (Fig. 7 C). Slope conductances derived from these plots are ~ 8 and 12.5 pS.

To compare these values with those reported from squid neurons, we derived a scaling factor to account for the higher $[K_i]$ used in the squid studies (Llano and Bookman, 1986; Llano et al., 1988; Perozo et al., 1991; Nealey et al., 1993). Slope g_K between +20 and +60 mV was compared for different $[K_i]$ values using inside-out patches from GFL neurons as illustrated in Fig. 7 D. A mean ratio of 1.6 ± 0.06 (SEM; $n = 3$) was determined for slope g_K in 470 mM K_i versus 140 mM K_i , as used in squid and oocyte experiments, respectively. When adjusted by this factor, the two unitary conductance values for SqKv1A are 13 and 20 pS. These values should be taken with some reservation, however, because the effects on g_K produced by sucrose and glycine, the compounds used to replace K, were not carefully determined.

Multiple single-channel current amplitudes for a defined Kv1 channel have been previously reported, but this feature has been attributed to substate-type behavior (Hoshi et al., 1994). In the case of SqKv1A, how-

ever, this does not seem to be the mechanism. Once these channels open they do not appear to switch directly between conductance levels (i.e., without an obvious closing as in Fig. 7 Biii). Because most of the patches we studied contained multiple channels, it is presently unclear whether a single channel can open to both amplitudes. One patch, which apparently contained a single channel, had only small conductance openings. Separate ensemble averages of sweeps containing only small conductance events or mixed events reveal that both types of channel activity inactivate on a time scale similar to that shown by macroscopic g_K in oocytes, GFL neurons (Fig. 6 B), and giant axons (Fig. 1 B). Although results in Fig. 8 suggest that the small conductance events may inactivate more rapidly and more completely than do the large events, this result must be regarded as tentative.

DISCUSSION

Several studies have attempted to determine the molecular identity of a K channel which underlies g_K in a native cell. Physical properties of native K channels closely resemble the properties of cDNA clones expressed in *Xenopus* oocytes in the case of T-lymphocytes (Grissmer et al., 1990; Grissmer et al., 1992), human myocardial cells (Fedida et al., 1993), GH3 cells (Myerhof et al., 1992), rat hippocampal neurons (Pardo et al., 1992), and in both *Aplysia* bag cells (Quattrochi et al., 1994) and the abdominal ganglion R15 neuron (Pfaffinger et al., 1991). In other cases, however, properties can differ significantly. For example, some biophysical properties of *Shaker* K channels expressed in heterologous systems are not shared by the homologous channels in *Drosophila* neurons (Zagotta et al., 1989). This is not surprising, because posttranslational modifications such as phosphorylation (Hoger et al., 1991; Covarrubias et al., 1994; Drain et al., 1994), cysteine oxidation (Ruppersberg et al., 1991), and subunit interactions (Rettig et al., 1994) can effect K channel behavior in dramatic ways, and any of these biochemical processes may differ between heterologous expression systems and the native cell type. Clearly, careful biophysical analysis alone may be insufficient to equate a cloned channel and its native counterpart.

In this paper we report the isolation of SqKv1A, and demonstrate that sequence corresponding to NH₂ and COOH termini and the channel core (S1-S6) is expressed in the somata GFL neurons. Because the SqKv1A cDNA was isolated as a single clone it is unlikely that an artificial, hybrid molecule has been constructed. RNase protection assays demonstrate that a probe specific to 5' coding and utr sequence (probe A) hybridizes only with GFL RNA whereas a probe specific to 3' coding and utr sequence (probe B) hybridizes to both SG and GFL RNA. This probably reflects the presence of a re-

lated K channel transcript (SqKv1B) expressed in SG neurons (Perri et al., 1994) that differs from SqKv1A in 5' coding and utr sequence, but is otherwise almost identical (manuscript in preparation). These structural differences suggest alternative splicing of a single gene, but this has not yet been proven.

Results of *in situ* hybridizations and RNase protection assays with probe A are particularly intriguing, because they suggest that the SqKv1A transcript may be specific for GFL neurons, although very low-level expression in SG neurons is extremely difficult to rule out. It is presently unknown if SqKv1A is expressed anywhere in the central nervous system.

Western blots with antibodies directed against SqKv1A confirm the presence of this channel in GFL and giant axon tissue samples. These blots also reveal two prominent bands in both tissues. The fusion protein used to make these antibodies contains sequence conserved in all Kv1 channels; it is therefore possible that a channel other than SqKv1A is responsible for either band on the Western blot. Extensive analysis of 70 Kv1 clones from our SG-GFL cDNA library has revealed the existence of several cDNAs closely related to SqKv1A, which may be splice variants, but none of these is expressed to an appreciable level in the GFL as determined by RNase protection (Perri et al., 1994). Other Kv1 genes may also exist. It is also possible that SqKv1A protein exists in two major forms due to differential post-translational modification. Phosphorylation is a likely candidate, because it has been shown to alter the voltage dependence of activation gating and inactivation of the squid 20 pS K channel (Perozo and Bezanilla, 1990; Perozo et al., 1991).

Although tissue samples from cleaned giant axons are necessarily contaminated with a substantial amount of material derived from the Schwann cell layer and remnant small axons, the possibility that the signal on the Western blot is due to SqKv1A expression in these cells is unlikely. *In situ* hybridizations clearly demonstrate that SqKv1A is expressed in GFL neurons and not in the elements which surround the giant axon as it exits the SG. Furthermore, the Western-blot banding pattern is similar, if not identical, in giant axon and GFL samples. Contamination from glial elements is expected to be much less in the latter source.

These molecular data are complemented by our physiological studies. Macroscopic I_K from oocytes injected with SqKv1A cRNA strongly resembles that in GFL neurons and giant axons. We therefore propose that the SqKv1A mRNA encodes the predominant K channel type in both preparations. Single channel studies lend further support to this proposition. A 20 pS channel predominates in GFL neurons and their giant axons and is thought to be "the main contributor to the delayed rectifier current" (Perozo et al., 1991). Single

SqKv1A channels show a similar unitary conductance and behavior. Two additional K channel types with unitary conductances of 10 and 40 pS have been reported from these neurons (Llano et al., 1988; Nealey et al., 1993), but their properties are not consistent with those of the macroscopic delayed rectifier current nor with SqKv1A. These channels may, however, contribute to the inactivation resistant component of I_K in the giant axon (Perozo et al. 1991) and GFL somata (see Fig. 6 E), and their molecular identification remains to be established.

Results presented in this report are contrary to the common belief that fast inactivation of macroscopic delayed rectifier g_K does not occur in the giant axon (Keynes, 1994). However, the few studies specifically designed to check for this phenomenon (Chabala, 1984; Clay, 1989) were carried out at low temperature, which greatly reduces the amount and extent of inactivation in both GFL cell bodies and giant axons (unpublished data). In addition, preliminary results indicate that fast inactivation in GFL neurons is labile and depends on several factors, including $[K_o]$ and the presence of internal Mg-ATP (Mathes et al., 1996). In this study we found axonal fast inactivation also to be variable and labile, but every experiment revealed its presence. Comparison of the extent of inactivation in cell bodies and giant axons is complicated by these sources of variability. A more complete description of inactivation of squid g_K and in SqKv1A channels is in preparation.

At present single channel studies cannot clarify whether the rate of inactivation of the 20 pS channel differs in cell bodies and giant axons. We have made preliminary single channel recordings from GFL cell bodies at 18°C that revealed outward unitary events with an amplitude consistent with that expected for the 20 pS channel (~ 2 pA at +20 mV) and with inactivation kinetics very similar to those shown by SqKv1A (see Fig. 8). These data are in agreement with those of Llano and Bookman (1986) who suggested that a single type of inactivating 20 pS K channel was responsible for macroscopic g_K in this preparation. Unfortunately, the most extensive single channel studies in GFL cell bodies have been performed using depolarized holding potentials (~ 0 mV; Nealey et al., 1993), making direct comparison with other data difficult. Furthermore, single channel recordings in giant axons held at negative voltages appear to have been limited to brief pulse durations (15 ms; Perozo et al., 1991), and the rate of inactivation in axonal 20 pS channels thus remains unclear.

Availability of the SqKv1A clone will permit detailed comparisons between the properties of this channel in its native environment and in heterologous expression systems. In this way the influence of a channel's local environment or posttranslational modifications on functional properties which differ between SqKv1A chan-

nels expressed in oocytes and the giant axon system may be better assessed. The relationship between the two SqKv1A unitary conductance events in oocytes is poorly understood. Do they represent two open states of the same channel molecule, or have some of the channels been modified to produce a distinct phenotype? Similarly, it is not known whether these two unitary event classes exist in GFL neurons or in giant axons in vivo. Additional analyses of SqKv1A in a suitable

expression system with the tools now available will help to identify those factors which induce the channel to display a particular unitary conductance, to determine whether other properties of the two unitary events classes differ (e.g., inactivation rate), and to elucidate the molecular and biochemical bases for this novel behavior. Unique features of the giant axon system will continue to be useful for extending these studies in vivo.

We thank Drs. C. M. Armstrong for carrying out experiments using the axial wire clamp and for valuable discussion, Z. Lebaric and S.R. Levinson for producing and characterizing the antisera used in this study, C. Mathes for performing whole-cell recordings on GFL neurons, M. Perri for help with RNase protection assays, and Mr. T. Liu for carrying out the in situ hybridization.

Initiation of molecular aspects of this work was enabled by an SGER award from the National Science Foundation (BNS-9006436); primary support was provided by National Institutes of Health grant NS-17510 (to W.F. Gilly) and Office of Naval Research N00014-93-1-0719 (AASERT for J. Rosenthal).

Original version received 20 March 1996 and accepted version received 24 June 1996.

REFERENCES

- Armstrong, C.M. 1969. Inactivation of the potassium conductance and related phenomena caused by quaternary ammonium ion injection in squid axons. *J. Gen. Physiol.* 54:553–575.
- Baker, P.F. 1984. The Squid Axon. Current Topics in Membranes and Transport. Vol. 22. Academic Press. Orlando, FL.
- Chabala, L.D. 1984. The kinetics of recovery and development of potassium channel inactivation in perfused squid (*Loligo pealei*) giant axons. *J. Physiol. (Camb.)* 356:193–220.
- Chomczynski, P., and N. Sacchi. 1987. Single-step method of RNA isolation by acid guanidinium thiocyanate-phenol-chloroform extraction. *Anal. Biochem.* 162:156–159.
- Clay, J.R. 1989. Slow inactivation and reactivation of the potassium channel in squid axons: a tail current analysis. *Biophys. J.* 55:407–414.
- Conti, F., and E. Neher. 1980. Single channel recordings of K⁺ currents in squid axons. *Nature (Lond.)* 285:140–143.
- Covarrubias, M., A. Wei, L. Salkoff, and T.B. Vyas. 1994. Elimination of rapid potassium channel inactivation by phosphorylation of the inactivation gate. *Neuron* 13:1403–1412.
- Drain, P., A.E. Dubin, and R.W. Aldrich. 1994. Regulation of Shaker K⁺ channel inactivation gating by the cAMP-dependent protein kinase. *Neuron* 12:1097–1109.
- Fedida, D., B. Wible, Z. Wang, B. Fermini, F. Faust, S. Nattel, and A.M. Brown. 1993. Identity of a novel delayed rectifier current from human heart with a cloned K⁺ channel current. *Circ. Res.* 73:210–216.
- Gilly, W.F., and C.M. Armstrong. 1982. Slowing of sodium channel opening kinetics in squid axon by extracellular zinc. *J. Gen. Physiol.* 79:935–964.
- Gilly, W.F., M.T. Lucero, and F.T. Horrigan. 1990. Control of the spatial distribution of sodium channels in giant fiber lobe neurons of the squid. *Neuron* 5:663–674.
- Grissmer, S., B. Dethleffs, J.J. Wasmuth, A.L. Goldin, G.A. Gutman, M.D. Cahalan, and K.G. Chandy. 1990. Expression and chromosomal localization of a lymphocyte potassium channel gene. *Proc. Natl. Acad. Sci. USA.* 87:9411–9415.
- Grissmer, S., S. Ghanshan, B. Dethleffs, J.D. McPherson, J.J. Wasmuth, G.A. Gutman, M.D. Cahalan, and K.G. Chandy. 1992. The shaw-related potassium channel gene, Kv3.1, on human chromosome 11, encodes the type 1 potassium channel in T cells. *J. Biol. Chem.* 267:20971–20979.
- Hodgkin, A.L., and A.F. Huxley. 1952. A quantitative description of membrane current and its application to conduction and excitation in nerve. *J. Physiol. (Camb.)* 117:500–544.
- Hoger, J.H., A.E. Walter, D. Vance, L. Yu, H.A. Lester, and N. Davidson. 1991. Modulation of a cloned mouse brain potassium channel. *Neuron* 6:227–236.
- Hoshi, T., W.N. Zagotta, and R.W. Aldrich. 1990. Biophysical and molecular mechanisms of Shaker potassium channel inactivation. *Science (Wash. DC)* 250:533–538.
- Hoshi, T., W.N. Zagotta, and R.W. Aldrich. 1994. Shaker potassium channel gating I: transitions near the open state. *J. Gen. Physiol.* 103:249–278.
- Jan, L.Y., and Y.N. Jan. 1992. Structural elements involved in specific potassium channel functions. *Annu. Rev. Physiol.* 54:537–555.
- Kamb, A., L.E. Iverson, and M.A. Tanouye. 1987. Molecular characterization of Shaker, a Drosophila gene that encodes a potassium channel. *Cell* 50:405–413.
- Keynes, R.D. 1994. The kinetics of voltage-gated ion channels. *Q. Rev. Biophys.* 27:339–434.
- Klumpp, D.J., E.J. Song, S. Ito, M.H. Sheng, L.Y. Jan, and L.H. Pinto. 1995. The Shaker-like potassium channels of the mouse rod bipolar cell and their contributions to the membrane current. *J. Neurosci.* 15:5004–5013.
- Kozak, M. 1989. The scanning model for translation: an update. *J. Cell Biol.* 108:229–244.
- Kyte, J., and R.F. Doolittle. 1982. A simple method for displaying the hydropathic character of a protein. *J. Mol. Biol.* 157:105–132.
- Li, M., Y.N. Jan, and L.Y. Jan. 1992. Specification of subunit assembly by the hydrophilic amino-terminal domain of the shaker potassium channel. *Science (Wash. DC)* 257:1225–1229.
- Liu, T.I., and W.F. Gilly. 1995. Tissue distribution and subcellular localization of Na⁺ channel mRNA in the nervous system of the squid, *Loligo opalescens*. *Receptors and Channels* 3:243–254.
- Llano, I., and R.J. Bookman. 1986. Ionic conductances of squid giant fiber lobe neurons. *J. Gen. Physiol.* 88:543–569.
- Llano, I., C.K. Webb, and F. Bezanilla. 1988. Potassium conductance of the squid giant axon. Single-channel studies. *J. Gen. Physiol.* 92:179–196.

- Mathes, C.M., J.J.C. Rosenthal, C.M. Armstrong, and W.F. Gilly. 1996. Similar potassium channel inactivation kinetics exist in squid giant axon and giant fiber lobe cell bodies. *Biophys. J.* 70: 188a. (Abstr.)
- Mi, H., T.J. Deerinck, M.H. Ellisman, and T.L. Schwarz. 1995. Differential distribution of closely related potassium channels in rat Schwann cells. *J. Neurosci.* 15:3761–3774.
- Mottes, J.R., and L.E. Iverson. 1995. Tissue-specific alternative splicing of hybrid Shaker/lacZ genes correlates with kinetic differences in Shaker K⁺ currents in vivo. *Neuron.* 14:613–623.
- Myerhof, W., J.R. Schwarz, C.K. Bauer, A. Hubel, and D. Richter. 1992. The rat pituitary tumour K⁺ channel expressed in frog oocytes induces a transient K⁺ current indistinguishable from that recorded in native cells. *J. Neuroendocrin.* 2:245–253.
- Nealey, T., S. Spires, R.A. Eatock, and T. Begenisich. 1993. Potassium channels in squid neuron cell bodies: comparison to axonal channels. *J. Membr. Biol.* 132:13–25.
- Pardo, L.A., S.H. Heinemann, H. Terlau, U. Ludewig, C. Lorra, O. Pongs, and W. Stuhmer. 1992. Extracellular potassium specifically modulates a rat brain potassium channel. *Proc. Natl. Acad. Sci. USA.* 89:2466–2470.
- Perozo, E., and F. Bezanilla. 1990. Phosphorylation affects voltage gating of the delayed rectifier K⁺ channel by electrostatic interactions. *Neuron.* 5:685–690.
- Perozo, E., F. Bezanilla, and R. Dipolo. 1989. Modulation of potassium channels in dialyzed squid axons: ATP-mediated phosphorylation. *J. Gen. Physiol.* 93:1195–1218.
- Perozo, E., D.S. Jong, and F. Bezanilla. 1991. Single channel studies of the phosphorylation of K⁺ channels in the squid giant axon. II. Nonstationary conditions. *J. Gen. Physiol.* 98:19–34.
- Perozo, E., C.A. Vandenberg, D.S. Jong, and F. Bezanilla. 1991. Single channel studies of the phosphorylation of K⁺ channels in the squid giant axon. I. Steady-state conditions. *J. Gen. Physiol.* 98:1–17.
- Perri, M.A., J.J.C. Rosenthal, T. Liu, and W.F. Gilly. 1994. Cloning and distribution of kv1 type potassium channel sequences in the squid stellate ganglia. *Biophys. J.* 66:105a. (Abstr.)
- Pfaffinger, P.J., Y. Furukawa, B. Zhao, D. Dugan, and E.R. Kandel. 1991. Cloning and expression of an Aplysia potassium ion channel and comparison with native Aplysia potassium ion currents. *J. Neurosci.* 11:918–927.
- Pongs, O. 1992. Molecular biology of voltage-dependent potassium channels. *Physiol. Rev.* 72:S69–S88.
- Proudfoot, N.J., and G.G. Brownlee. 1976. 3' non-coding region sequences in eukaryotic messenger RNA. *Nature (Lond.).* 263: 211–214.
- Quattrochi, E.A., J. Marshall, and L.K. Kaczmarek. 1994. A Shab potassium channel contributes to action potential broadening in peptidergic neurons. *Neuron.* 12:73–86.
- Rettig, J., S.H. Heinemann, F. Wunder, C. Lorra, D.N. Parcej, J.O. Dolly, and O. Pongs. 1994. Inactivation properties of voltage-gated K⁺ channels altered by presence of beta-subunit. *Nature (Lond.).* 369:289–294.
- Ribera, A.B., and D.A. Nguyen. 1993. Primary sensory neurons express a shaker-like potassium channel gene. *J. Neurosci.* 13:4988–4996.
- Rosenberg, A.H., B.N. Lade, D.S. Chui, S.W. Lin, J.J. Dunn, and F.W. Studier. 1987. Vectors for selective expression of cloned DNAs by T7 RNA polymerase. *Gene.* 56:125–135.
- Rosenthal, J.C., M.A. Perri, and W.F. Gilly. 1995. Expression of two k channel mRNAs from cloned squid sequences. *Biophys. J.* 68: 270a. (Abstr.)
- Rosenthal, J.J.C., and W.F. Gilly. 1993. Amino acid sequence of a putative sodium channel expressed in the giant axon of the squid *Loligo opalescens*. *Proc. Natl. Acad. Sci. USA.* 90:10026–10030.
- Ruppersberg, J.P., M. Stocker, O. Pongs, S.H. Heinemann, R. Frank, and M. Koenen. 1991. Regulation of fast inactivation of cloned mammalian IK(A) channels by cysteine oxidation. *Nature (Lond.).* 352:711–714.
- Sambrook, J., E.F. Fritsch, and T. Maniatis. 1989. Molecular Cloning: A Laboratory Manual. 2nd ed. Cold Spring Harbor Laboratory Press. Cold Spring Harbor, New York.
- Schwarz, T.L., D.M. Papazian, R.C. Carretto, Y.N. Jan, and L.Y. Jan. 1990. Immunological characterization of K⁺ channel components from the Shaker locus and differential distribution of splicing variants in Drosophila. *Neuron.* 4:119–127.
- Schwarz, T.L., B.L. Tempel, D.M. Papazian, Y.N. Jan, and L.Y. Jan. 1988. Multiple potassium-channel components are produced by alternative splicing at the shaker locus in drosophila. *Nature (Lond.).* 331:137–142.
- Sheng, M., M.L. Tsaur, Y.N. Jan, and L.Y. Jan. 1992. Subcellular segregation of two A-type K⁺ channel proteins in rat central neurons. *Neuron.* 9:271–284.
- Sheng, M., M.L. Tsaur, Y.N. Jan, and L.Y. Jan. 1994. Contrasting subcellular localization of the Kv1.2 K⁺ channel subunit in different neurons of rat brain. *J. Neurosci.* 14:2408–2417.
- Simmons, D.M., J.L. Arriza, and L.W. Swanson. 1989. A complete protocol for in situ hybridization of messenger RNAs in brain and other tissues with radio-labeled single-stranded RNA probes. *J. Histochemol.* 12:169–181.
- Stühmer, W., J.P. Ruppersberg, K.H. Schroeter, B. Sakmann, M. Stocker, K.P. Giese, A. Perschke, A. Baumann, and O. Pongs. 1989. Molecular basis of functional diversity of voltage-gated potassium channels in mammalian brain. *EMBO (Eur. Mol. Biol. Organ.) J.* 8:3235–3244.
- Tsaur, M.L., M. Sheng, D.H. Lowenstein, Y.N. Jan, and L.Y. Jan. 1992. Differential expression of K⁺ channel mRNAs in the rat brain and down-regulation in the hippocampus following seizures. *Neuron.* 8:1055–1067.
- Tseng-Crank, J., J.A. Yao, M.F. Berman, and G.N. Tseng. 1993. Functional role of the NH₂-terminal cytoplasmic domain of a mammalian A-type K channel. *J. Gen. Physiol.* 102:1057–1083.
- Wang, H., D.D. Kunkel, T.M. Martin, P.A. Schwartzkroin, and B.L. Tempel. 1993. Heteromultimeric potassium channels in terminal and juxtaparanodal regions of neurons. *Nature (Lond.).* 365:75–79.
- Wang, H., D.D. Kunkel, P.A. Schwartzkroin, and B.L. Tempel. 1994. Localization of Kv1.1 and Kv1.2, two K channel proteins, to synaptic terminals, somata and dendrites in the mouse brain. *J. Neurosci.* 14:4588–4599.
- Wei, A., M. Covarrubias, A. Butler, K. Baker, M. Pak, and L. Salkoff. 1990. Potassium current diversity is produced by an extended gene family conserved in Drosophila and mouse. *Science (Wash. DC).* 248:599–603.
- Zagotta, W.N., S. Germeraad, S.S. Garber, T. Hoshi, and R.W. Aldrich. 1989. Properties of ShB A-type potassium channels expressed in Shaker mutant Drosophila by germline transformation. *Neuron.* 3:773–782.